Numerical analysis of wave processes under high-speed impact on an object from CFRP

M. Khudorozhko[1,2*], *E.* Fomina[1,2], *A.* Dumansky[1,2], and *Hao* Liu[1]

[1]Bauman Moscow State Technical University, 2nd Baumanskaya str., 105005 Moscow, Russia
[2]Mechanical Engineering Research Institute of the Russian Academy of Sciences, 4 Maly Kharitonyevsky Pereulok, 119991 Moscow, Russia

Abstract. Numerical simulation of the impact of an aluminum particle on a composite medium was carried out. Carbon fiber reinforced plastic (CFRP) laminates T300/69 were used as a research object. The behavior of CFRP was analyzed at an impact velocity of 11 km/s and an aluminum particle mass of 1 g. The composite layers were located in planes oriented perpendicular to the direction of reinforcement. The Smoothed-particle hydrodynamics (SPH) method in conjunction with Ansys Autodyn was used for numerical modeling. Since large deformations and fracture of the objects were observed at such high impact velocities, which indicated a violation of the continuity of the material, that makes it incorrect to use of traditional mesh methods. The dependence of the shock wave propagation velocities in CFRP on time was obtained. The minimum thickness of the protective screen made of CFRP was estimated. **Key words:** space debris, carbon fiber reinforced plastic, shock waves, Smoothed-particle hydrodynamics method, sound velocity.

1 Introduction

Polymer composite materials, such as CFRP, have found wide application in aviation and aerospace due to high values of physical and mechanical characteristics. The combination of T300/69 with a strength of about 1500 MPa, an elastic modulus of 130 GPa and a low-density of 1560 kg/m^3 makes it possible to use CFRP as protective structures in near-Earth space. As is known, one of the dangerous factors in orbit for spacecrafts is space debris, a collision with which may lead to both partial and complete failure of the structure. The question arises about the behavior of materials and structures when colliding with such objects in space. Modern test facilities do not yet allow to achieve an impact velocity of more than 11 km/s [1]. Thus, numerical and theoretical calculations are the only way to assess the strength of structures. As studies have showed that the deformation curves, as well as the strength properties of the material, significantly differ at various loading velocities [2].

Even more important thing is the anisotropic behavior composite materials [3-6]. In particular, upon impact, energy transfer through the material in the form of wave processes will inevitably occur. At the same time, the speed of propagation of waves varies in different directions, as well as the speed of propagation of longitudinal and transverse waves. The

* Corresponding author: khudorozko.mixa@gmail.com

study of elastic wave propagation in CFRP contributes to the development of methods of non-destructive testing of finished products [7, 8]. However, in addition to these features, it is important to know that the impact velocity in most cases exceeds the speed of sound in the material, which leads to a qualitative difference in the results. Besides, researchers have identified new ones. For example, experimental data on the propagation of shock waves in a composite material consisting of aramid fibers and an epoxy matrix are presented in [9]. As a result of the study, the authors concluded that the impact compressibility of the material practically didn't depend on the orientation of the fibers. In [10], the effect of impact on fiberglass with E-glass and C-glass fibers was analyzed. Data analysis has shown that for a material with a large modulus of elasticity, it has the greater impact resistance. In [11], the processes of damage and destruction of a two-layer ceramic and aluminum plate caused by impact were analyzed. The impact was simulated in the software Ansys Autodyn. As a result, it was shown that the use of metal-ceramic composites makes it possible to increase the effectiveness of the protective screen. In [12], a simulation of an impact into a composite-coated plate using the SPH method was carried out and compliance with the experiment was shown. A similar study of sandwich panels and fiberglass was carried out in [13]. In the paper [14] presents a model of CFRP that takes into account elastic-plastic damage and the behavior of the material in the experiment corresponded to the presented model. The behavior of fiberglass at relatively low interaction rates is presented in [15], in which a numerical analysis of the impact of an aluminum particle on a CFRP object using SPH method is carried out.

2 Description of mathematical model

Upon the impact with the indicated values of particle's velocities and masses large ruptures and splinters will occur in the used materials, which indicates the violation of the continuity hypothesis of the medium. Accounting to this fact, the calculation was carried out using the meshfree SPH method. This method is used in works [11, 12, 16]. The essence of this method is to represent the body as a collection of a large number of particles. In essence, this method is completely discrete, while grid methods, for example, the finite element method, only approximate the solution of a differential equation by finite increments of parameters. The determining relations for this method are based on the laws of conservation of mass, momentum and energy. The value of a parameter for a point with index i is calculated based on the parameter values at points with index j located at some distance from this point according to the following relations:

$$\rho_i = \sum_j m_j \cdot W_{ij}(h) \tag{1}$$

$$\frac{dU_i}{dt} = -\sum_j \frac{m_j}{\rho_i \cdot \rho_j} \cdot \left(\sigma_j - \sigma_i\right) \cdot \nabla W_{ij}(h) \tag{2}$$

$$\frac{dE_i}{dt} = -\sum_j \frac{m_j}{\rho_i \cdot \rho_j} \cdot \left(U_j - U_i\right) \cdot \sigma_i \cdot \nabla W_{ij}(h) \tag{3}$$

Where ρ_i – particle density, m_j – particle mass, U_i – particle velocity, σ_i – stress tensor, E_i – particle energy, W_{ij} – kernel function. The core function has the dimension of the inverse volume and expresses the degree of influence depending on the distance from the rest of the particles. The choice of the kernel function is left to the researcher. The most common

variants of the kernel function are presented in [17, 18]. When modeling the impact, the core function in the form of a cubic spline was used:

$$W_{ij}(h) = \frac{1}{\pi h^3}\begin{cases} 1 - \frac{3}{2}v^2 + \frac{3}{4}v^3 & 0 < v < 1 \\ \frac{1}{4}(2-v)^3 & 1 \le v < 2 \\ 0 & 2 \le v \end{cases} \qquad v = \left|r_j - r_i\right| \tag{4}$$

Equations (1) - (3) are a system of algebraic and differential equations that are solved jointly and sequentially for each particle at each time step, based on the given initial and boundary conditions. Numerical integration is carried out according to an explicit scheme with a given time step. Since the material is considered homogeneous, the mass of the particles is determined from the obvious ratio:

$$m_i = \frac{M}{N} \tag{5}$$

Where N – number of particles, M – body weight.

Such a system of equations does not imply an explicit assignment and description of wave processes in the material upon impact, however, as a result of solving these equations, waves are nevertheless formed. The analysis was carried out using the consequences of the Rankine-Hugonio relations [19, 20].

3 Problem statement

The numerical solution was carried out using the software Ansys Autodyn. The initial model was a parallelepiped made of the CFRP with dimensions of 25x25x50mm and an aluminum cube weighing 1g with an edge size of 0.7 mm. The initial velocity of the aluminum particle is 11 km/s. During the solution, the maximum time step was assumed to be $4 \cdot 10^{-9}\ s$. The values of the characteristics of high-strength CFRP laminates are taken from [21] and are given in table №1. The material was assumed to be transversally isotropic.

Table 1. Physical and mechanical characteristics of CFRP T300/69.

ρ [kg/m^3]	1560
E_1 [GPa]	140
E_2 [GPa]	9.0
G_{12} [GPa]	4.6
v_{12}	0.32
v_{31}	0.28
X_t [MPa]	1700
Y_t [MPa]	51
X_c [MPa]	1100
Y_c [MPa]	130
S_{12} [MPa]	70

CFRP is considered to be perfectly elastic until the failure. The Tsai-Hill relations are used as a strength theory [22]. The composite layers are located in planes oriented at 90° to the plane of impact.

The aluminum is modeled taking into account the behavior under high-speed impact. The Mie-Grüneisen equation [20] of state is applied:

$$p = p_0 + \Gamma \cdot \rho \cdot (e - e_0) \quad (6)$$

Where p – material pressure, ρ – density, e – internal energy, Γ – Grüneisen parameter. The parameters of this equation are determined automatically by the program, based on the empirically established relationship between the velocity of the shock wave and the velocity of the particles of the medium:

$$U_s = C_0 + S \cdot u_p \quad (7)$$

Where U_s – shock velocity, C_0 – sound velocity, S – constant, u_p – velocity of medium particles. The numerical values of the parameters for aluminum are presented in the table №2.

Table 2 – Aluminum properties

ρ [kg/m^3]	2785
C_0 [km/s]	5.32
S	1.34
Γ	2

This statement of the problem does not take into account:

- The microstructure of the composite
- Features of interlayer interaction
- Dependence of material characteristics on temperature and loading speed
- Phase transitions due to temperature rise during impact

In this calculated case, the impact velocity exceeds the propagation velocity of the sound wave in CFRP. Thus, it is expected that the velocity of the shock wave at the beginning will be determined by the velocity of the aluminum particle. When the speed of the aluminum particle becomes equal to the speed of sound in CFRP, the shock wave should be disrupted. Since the material is orthotropic, the speed of sound also depends on the direction. In the adiabatic approximation, the speed of sound in the material can be estimated as follows:

$$C_{||} = \sqrt{\frac{E_1}{\rho}} = 10.7\ \frac{km}{s}\ ;\ C_{\perp} = \sqrt{\frac{E_2}{\rho}} = 4.0\ \frac{km}{s}\ ;\ C_v = \sqrt{\frac{K}{\rho}} = 7.7\ \frac{km}{s}$$

Where $C_{||}$, $C_{\perp}$, C_v – the speed of sound along the direction of fiber laying, across and volume velocity, respectively, E_1, E_2, K – elastic modulus along the fibers, across and volumetric modulus, respectively, ρ – material density.

4 Analysis of results

Figure 1 shows the penetration of an aluminum particle into the barrier of CFRP T300/69. The aluminum particle is noticeably flattened and experiences plastic deformations. It is observed that the slowest sections of aluminum are located near the contact zone with the barrier of CFRP T300/69.

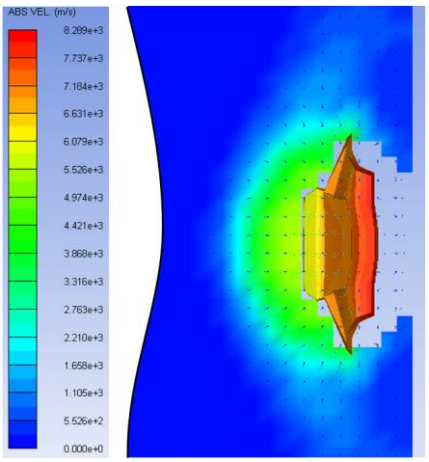

Fig. 1. Velocity distribution

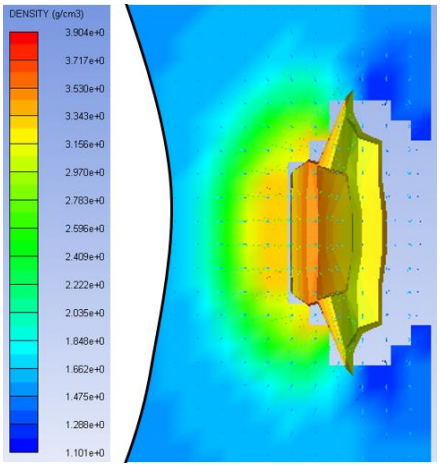

Fig. 2. Density distribution.

Figure 2 shows the density distribution of a plastically deformable impactor and a CFRP barrier. It can be seen that the maximum density value is located near the contact zone. Based on the Rankine-Hugonio ratios for mass conservation, the calculated and calculated density in the impact zone:

Estimated

$$\rho_1 = 3580\ \frac{kg}{m^3}$$

Numerical simulation

$$\rho_1 = 3498\ \frac{kg}{m^3}$$

The dependence of the shock wave velocity in the CFRP barrier on time is obtained. The method of constructing the dependence of the wave velocity on time is shown as follows:

- The values of the velocities V of points in the CFRP object along the direction of impact are determined. The points are located along the direction of impact in 5 mm increments from 0 to 25 mm in thickness (Fig. 3)
- The time when the speed of the point reached the extremum is determined
- The distance between the points is divided by the time defined in the previous step

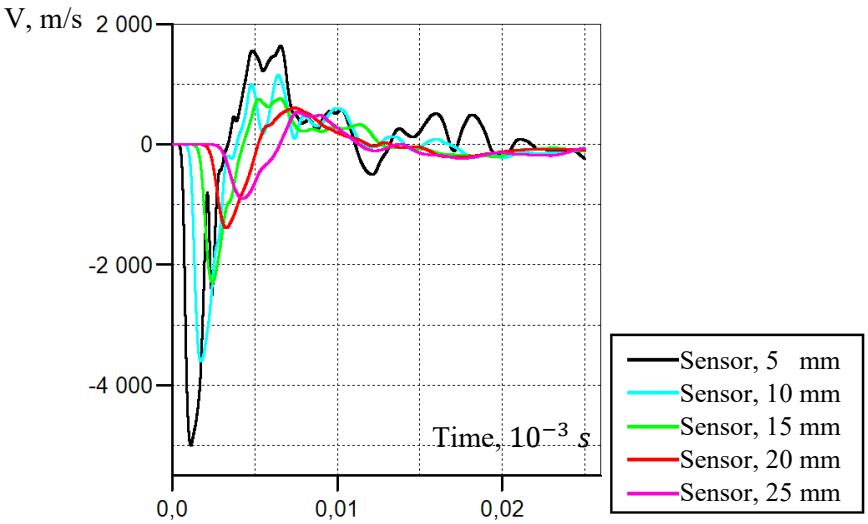

Fig. 3. Velocities of points along the direction of impact.

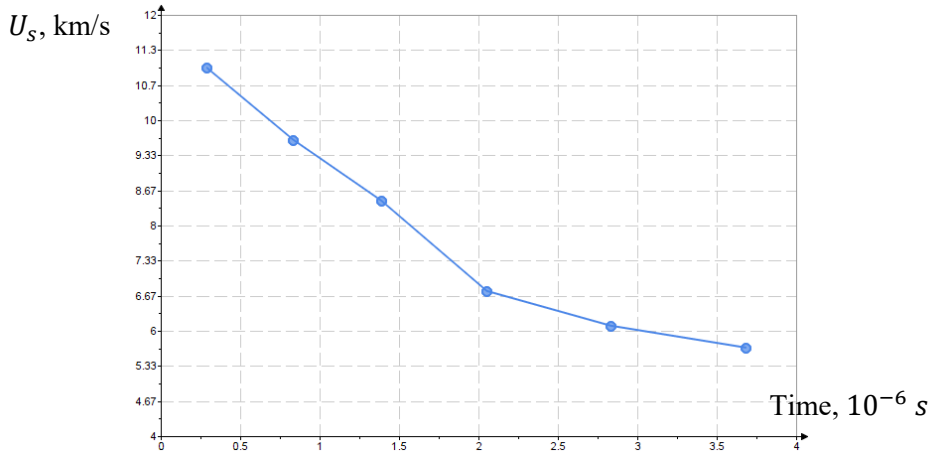

Fig. 4. Dependence of the shock wave velocity on time.

The obtained dependence of the shock wave velocity U_s on time is shown in the figure 4. The values of the velocities of the points over time asymptotically tended to zero. The obtained dependence of the shock wave velocity U_s on time is shown in Figure 4. The graph shows that the shock wave velocity fades over time. Thus, taking into account the errors caused by the approximations of the computational model, the estimate of the shock wave disruption time is approximately $1.7 \cdot 10^{-6}$ s. We assume that when this velocity is reached, the particle will not move further into the CFRP object. The dependence of the wave velocity on time can be considered linear up to the point of separation of the wave. In this case, the estimate of the penetration depth of the aluminum particle is 13,5 mm.

Figures 5 and 6 show the velocity distributions of the CFRP particles at different time points equal to $1.96 \cdot 10^{-6}$ s and $2.46 \cdot 10^{-6}$ s, respectively. The shock wave disruption zone is located inside a red circle highlighted in red. The simulation results are consistent with the experimental results obtained in [9]. The critical velocity for the disruption of the shock wave is the volume velocity of sound in the material.

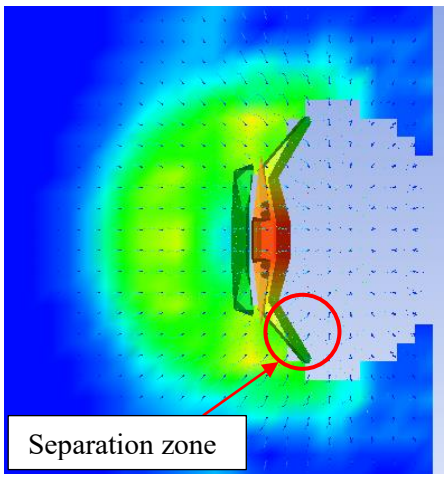

Fig. 5. Velocity distribution. Time – $1.96 \cdot 10^{-6}$ s.

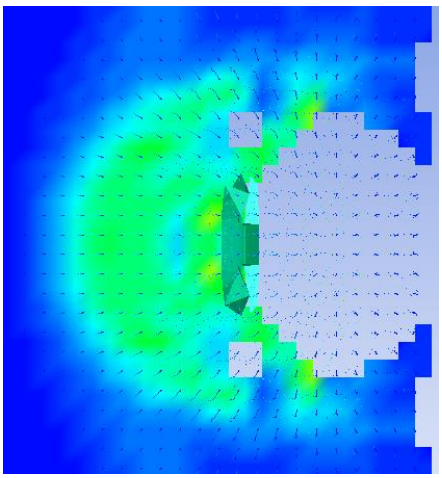

Fig. 6. Velocity distribution. Time – $2.46 \cdot 10^{-6}$s.

5 Conclusions

A numerical analysis of wave processes under the high-speed impact of an aluminum particle on a CFRP object using the SPH method in conjunction with Ansys Autodyn was carried out. The critical velocity of the shock wave at which wave separates from particle was equal to the volumetric velocity of sound in the material. The dependence of the velocity of the shock wave in the CFRP object on time was obtained, according to which it is possible to estimate the penetration depth of the impactor into the CFRP object. As a result of the calculation, supposing the dependence of the shock wave velocity on time is linear, for an impact velocity of 11 km/s the aluminum particle penetration depth estimated to be equal to 13.5 mm. It is obvious, in order to meet the protection conditions the thickness of the protective shield must exceed the obtained value. It is shown that the effectiveness of protective screens increases by using high-modulus materials.

References

1. K.V. Mikhailovskii, S.V. Reznik, P.V.Prosuntsov, AIP Conference Proceedings **2171(1)**, 030017 (2019)
2. A. Dumansky, H. Liu, M. Alimov, MATEC Web of Conferences **329**, 03048 (2020
3. A.H. Orta, J. Vandendriessche, M. Kersemans et al, Ultrasonics **116**, 106482 (2021)
4. A. Mardanshahi, V. Nasir, S. Kazemirad, M.M. Shokrieh, Composite Structures **246**, 112403 (2020)
5. M.S. Meon, J.B. Saedon, S. Shawal, H. Husain, et al. IOP Conference Series: Materials Science and Engineering **1092(1)**, 012043 (2021)
6. C. Wang, T. Ren, Y. Miao, T. Suo et al, Composite Structures **246**, 112392 (2020)
7. S.V. Kuznetsov, Composite Structures **290**, 115532 (2022)
8. S.V. Bochkarev, A.F. Salnikov, A.L. Galinovsky, Mechanics of Composite Materials **57(6)**, 759-768 (2022)
9. V. Mochalova, A. Utkin, A. Savinykh, G. Garkushin, Composite Structures **273**, 114309 (2021)
10. N. Razali, M.T.H. Sultan, F. Cardona, IOP Conference Series: Materials Science and Engineering **152**, 012045 (2016)
11. S. Ren, R. Long, Q. Zhang, C. Chen, International Journal of Impact Engineering **148**, 103759 (2021)
12. P. Shojaei, M. Trabia, B. O'Toole, R. Jennings et al, Composites Part B: Engineering **194**, 108068 (2020)
13. R.C. Tennyson, C.G. Lamontagne, *Impact Behaviour of Fibre-Reinforced Composite Materials and Structures* (Woodhead Publishing, 2000)
14. H. Liu, J. Liu, Y. Ding, Z.E. Hall et al, Composites Part B: Engineering **201**, 108389 (2020)
15. A.A. Nassr, T. Yagi, T. Maruyama, G. Hayashi, International Journal of Impact Engineering **111**, 21-33 (2018)
16. S. Zhao, Z. Song, H.D. Espinosa, International Journal of Impact Engineering **144**, 103586 (2020)
17. Randles P.W. L.D. Libersky Computer Methods in Applied Mechanics and Engineering **139(1)**, 375-408 (1996)

18. J.W. Swegle, D.L. Hicks, S.W. Attaway, Journal of Computational Physics **116(1)**, 123-134 (1995)
19. D.F. Vogl, D. Langmayr, N.V. Erkaev, H.K. Biernat et al, Planetary and Space Science **51(12)**, 715-722 (2003)
20. G.I. Kanel, S.V. Razorenov, A.V. Utkin, V.E. Fortov, *Shock-wave phenomena in condensed media* (Janus-K, M., 1996)
21. J. Liu, Y. Xu, X. Yi, T. Wei, Composite Structures **280**, 114887 (2022)
22. J. Gawryluk, A. Teter, Composite Structures **269**, 114046 (2021)